

# Thermodynamic Properties of the One-Dimensional Extended Quantum Compass Model in the Presence of a Transverse Field

R. Jafari<sup>1,2</sup>

<sup>1</sup>*Research Department, Nanosolar System Company (NSS), Zanjan 45158-65911, Iran\**

<sup>2</sup>*Department of Physics, Institute for Advanced Studies in Basic Sciences (IASBS), Zanjan 45137-66731, Iran*

(Dated: June 13, 2022)

The presence of a quantum critical point can significantly affect the thermodynamic properties of a material at finite temperatures. This is reflected, *e.g.*, in the entropy landscape  $S(T, c)$  in the vicinity of a quantum critical point, yielding particularly strong variations for varying the tuning parameter  $c$  such as magnetic field. In this work we have studied the thermodynamic properties of the quantum compass model in the presence of a transverse field. The specific heat, entropy and cooling rate under an adiabatic demagnetization process have been calculated. During an adiabatic (de)magnetization process temperature drops in the vicinity of a field-induced zero-temperature quantum phase transitions. However close to field-induced quantum phase transitions we observe a large magnetocaloric effect.

PACS numbers: 75.10.Pq; 75.30.Sg; 02.70.-c

## I. INTRODUCTION

The magnetocaloric effect (MCE), in general, addresses the change of temperature of magnetic systems under the adiabatic variation of an external magnetic field which was discovered in iron by Warburg in 1881<sup>1</sup>. The MCE has been widely used for refrigeration due to potential room-temperature cooling applications<sup>2,3</sup>. For example, adiabatic demagnetization of paramagnetic salts was the first method to reach temperatures below 1K<sup>4</sup> whereas demagnetization of nuclear spins has reached temperatures down to 100pK<sup>5</sup> and is still the method of choice for  $\mu$ K-range cooling<sup>6</sup>. The cooling rate at the adiabatic demagnetization ( $\frac{\partial T}{\partial h}$ ) for an ideal paramagnet (*i.e.*, a system of non-interacting magnetic moments) is equal to  $T/H$ , which means linear monotonic dependence of temperature on strength of the magnetic field. This linear dependence rise out of a direct consequence of the fact that for any paramagnetic system the entropy depends only on the ratio  $T/H$ , so for any isentrope one gets  $H/T = \text{const.}$  However, the matter could undergo crucial changes in systems with interacting spins. For instance, in ferromagnets near the Curie point one can observe a substantial enhancement of the effect<sup>3</sup>.

As has been shown in early investigations, quantum antiferromagnets are more efficient low-temperature magnetic coolers than ferromagnets<sup>7</sup>. This fact is connected with the behavior of the entropy of antiferromagnets. The entropy of any antiferromagnet at low temperatures displays (at least) one maximum as a function of magnetic field, which usually, according to the third law of thermodynamics, falls to zero at  $T \rightarrow 0$ .

However, the MCE in quantum spin systems has recently attracted scientists attention. From one hand, field-induced quantum phase transitions lead to universal responses when the applied field is varied adiabatically<sup>8-11</sup>. On the other hand, it was observed

that the MCE is enhanced by geometric frustration<sup>12-15</sup>, promising improved efficiency in low-temperature cooling applications. More generally, the MCE is particularly large in the vicinity of quantum critical points (QCPs). The MCE is closely related to the generalized Grüneisen ratios

$$\Gamma_c = -\frac{1}{T} \frac{(\partial S / \partial C)_T}{(\partial S / \partial T)_c},$$

where  $c$  is the control parameter governing the quantum phase transition which would be external magnetic field  $h$  for MCE. Using basic thermodynamic relations<sup>3</sup>, the generalized Grüneisen ratio  $\Gamma_h$  can be related to the adiabatic cooling rate  $(\partial T / \partial H)_S$ <sup>16</sup>

$$\Gamma_h = \frac{1}{T} \left( \frac{\partial T}{\partial h} \right)_S = -\frac{1}{C_c} \left( \frac{\partial M}{\partial T} \right)_h.$$

The magnetic cooling rate is an important quantity for the characterization of quantum critical points (QCPs), *i.e.*, quantum phase transitions between different magnetic structures under tuning the magnetic field at  $T = 0$ .

Quantum Compass Model (QCM) is simplified model which describes the nature of the orbital states in the case of a twofold degeneracy<sup>17</sup>. Originally, the QCM has been used to describe the Mott insulators with orbit degeneracies. It depends on the lattice geometry and belongs to the low energy Hamiltonian originated from the magnetic interactions in Mott-Hubbard systems with the strong spin-orbit coupling<sup>18</sup>. In QCM the orbital degrees of freedom are represented by pseudospin operators and coupled anisotropically in such a way as to mimic the competition between orbital orderings in different directions. For simplicity, the one-dimensional (1D) QCM, is constructed by antiferromagnetic order of  $X$  and  $Y$  pseudospin components on odd and even bonds, respectively<sup>19,20</sup>. Moreover, the extended version of the 1D QCM, is obtained by introducing one more tunable parameter, has been studied by Eriksson *et al.*<sup>21</sup>.

To the best of our knowledge, thermodynamic properties of the extended version of 1D QCM in a transverse field has not been studied so far. Since the extended QCM shows two critical lines (first order and second order transition lines), investigation on its thermodynamic properties and MCE will be of great importance. However, in our recent work, we have shown that extended QCM in a transverse field reveals a rich phase diagram which includes several critical surfaces depending on exchange couplings<sup>22</sup>. In this paper we exploit the method employed in Refs. [20] and [22] to investigate thermodynamic properties of extended QCM in absent and presence of a transverse magnetic field.

## II. HAMILTONIAN AND EXACT SOLUTION

Consider the Hamiltonian

$$H = \sum_{n=1}^{N'} [J_1 \sigma_{2n-1}^x \sigma_{2n}^x + J_2 \sigma_{2n-1}^y \sigma_{2n}^y + L_1 \sigma_{2n}^x \sigma_{2n+1}^x + h_1 \sigma_{2n-1}^z + h_2 \sigma_{2n}^z]. \quad (1)$$

where  $J_1$  and  $J_2$  are the odd bonds exchange couplings,  $L_1$  is the even bond exchange coupling and the parameters  $h_1$  and  $h_2$  describe the external magnetic field at the even and odd lattice sites respectively which its alternating nature is assumed to arise from different magnetic moments or different g-factors of the spin. The number of sites is  $N = 2N'$  and for simplicity we assume periodic boundary conditions. The above Hamiltonian (Eq. (1)) can be exactly diagonalized by standard Jordan-Wigner transformation<sup>23,24</sup> as defined below,

$$\sigma_j^x = b_j^+ + b_j^-, \quad \sigma_j^y = b_j^+ - b_j^-, \quad \sigma_j^z = 2b_j^+ b_j^- - 1$$

$$b_j^+ = c_j^\dagger e^{i\pi \sum_{m=1}^{j-1} c_m^\dagger c_m}, \quad b_j^- = e^{-i\pi \sum_{m=1}^{j-1} c_m^\dagger c_m} c_j$$

which transforms spins into fermionic operators  $c_j$ .

The crucial step is to define independent Majorana fermions<sup>25</sup> at site  $n$ ,  $c_n^q \equiv c_{2n-1}$  and  $c_n^p \equiv c_{2n}$ . This can be regarded as quasiparticles' spin or as splitting the chain into bi-atomic elementary cells<sup>20</sup>.

Substituting for  $\sigma_j^x$ ,  $\sigma_j^y$  and  $\sigma_j^z$  ( $j = 2n, 2n-1$ ) in terms of Majorana fermions with antiperiodic boundary condition (subspace with even number of fermions) followed by a Fourier transformation, Hamiltonian Eq. (1) (apart from additive constant), can be written as

$$H^+ = \sum_k \left[ J c_k^{q\dagger} c_{-k}^{p\dagger} + L c_k^{q\dagger} c_k^p + 2h_1 c_k^{q\dagger} c_k^q + 2h_2 c_k^{p\dagger} c_k^p + h.c. \right],$$

where  $J = (J_1 - J_2) - L_1 e^{ik}$ ,  $L = (J_1 + J_2) + L_1 e^{ik}$  and  $k = \pm \frac{j\pi}{N'}$ , ( $j = 1, 3, \dots, N' - 1$ ).

It should be pointed out that though the GS in periodic and antiperiodic boundary conditions are slightly different in the finite-size system, they are identical in the thermodynamic limit and the essential features in finite size are also not altered qualitatively.

Finally, diagonalization is completed by a four-dimensional Bogoliubov transformation connecting  $c_k^{q\dagger}$ ,  $c_{-k}^q$ ,  $c_k^{p\dagger}$ ,  $c_{-k}^p$  and one thus obtains two different kind of quasiparticles,

$$H = \sum_k \left[ E_k^q (\gamma_k^{q\dagger} \gamma_k^q - \frac{1}{2}) + E_k^p (\gamma_k^{p\dagger} \gamma_k^p - \frac{1}{2}) \right], \quad (2)$$

where  $E_k^q = \sqrt{2(a+c)}$  and  $E_k^p = \sqrt{2(a-c)}$ ,  $c = \sqrt{a^2 - b}$  in which

$$\begin{aligned} a &= h_1^2 + h_2^2 + J_1^2 + J_2^2 + L_1^2 + 2L_1 J_2 \cos k, \\ b &= 4[(J_1 J_2 - h_1 h_2)^2 + 2J_1 L_2 (J_1 J_2 - h_1 h_2) \cos k + J_1^2 L_2^2]. \end{aligned}$$

The ground state ( $E_G$ ) and the lowest excited state ( $E_E$ ) energies are obtained from Eq.(3),

$$E_G = -\frac{1}{2} \sum_k (E_k^q + E_k^p), \quad E_E = -\frac{1}{2} \sum_k (E_k^q - E_k^p),$$

which can be written as a function of  $a$  and  $b$ ,

$$E_G = -2 \sum_{k>0} \sqrt{a + \sqrt{b}}, \quad E_E = -2 \sum_{k>0} \sqrt{a - \sqrt{b}} \quad (3)$$

It is clear that the ground state is separated from the lowest energy pseudospin excitation by a pseudospin gap  $\Delta = |E_E - E_G|$ , which vanishes at  $h_1 h_2 = J_1 (J_2 \pm L_1)$  in the thermodynamic limit.

It should be mentioned that the exact spectrum and the pseudospin gap are the same as that obtained in our recent work for  $h_1 = h_2 = h$ <sup>22</sup>.

For investigation on the thermodynamic properties of the model, we have calculated the free energy per sit.

$$f = -\frac{1}{\beta} \lim_{N \rightarrow \infty} \left[ \frac{1}{N} \ln Sp \exp(-\beta H) \right], \quad (4)$$

where  $Sp$  means a summation over all occupation patterns. The free energy is easily obtained by using the diagonalized quadratic form of  $H$  (Eq.(2)),

$$f = -\frac{1}{\beta} \frac{1}{2\pi} \int_{-\pi}^{\pi} \ln \left[ 2 \cosh \left( \frac{\beta(E_k^q + E_k^p)}{2} \right) + 2 \cosh \left( \frac{\beta(E_k^q - E_k^p)}{2} \right) \right] dk \quad (5)$$

Entropy ( $S$ ), specific heat ( $C_v$ ) and the normalized cooling rate ( $\Gamma_c$ ) are related to free energy via a simple thermodynamic relation,

$$S = \beta^2 \frac{\partial f}{\partial \beta}, \quad C_v = -\beta \frac{\partial S}{\partial \beta}, \quad \Gamma_c = -\frac{\partial^2 f}{\partial T \partial c} / (T \frac{\partial^2 f}{\partial T^2}).$$

Then, from the Eq.(5) one can easily obtain simple analytic expressions for all thermodynamic functions of the system. The adiabatic demagnetization curves can be found from a direct solution of  $S(c, T) = \text{const.}$

### III. EXTENDED QUANTUM COMPASS MODEL IN A HOMOGENOUS MAGNETIC FIELD ( $h_1 = h_2 = h$ )

In our recent work, we have investigated the phase diagram of the extended quantum compass model in homogenous transverse field by use of the gap analysis and universality of derivative of the correlation functions (ground state)<sup>22</sup>. This model is always gapful except at the critical surfaces where the energy gap disappears. We have obtained the analytic expressions for all critical fields which drive quantum phase transitions (QPT) as a function of exchange couplings,  $h_0 = \sqrt{J_1(J_2 + L_1)}$ ,  $h_\pi = \sqrt{J_1(J_2 - L_1)}$ .

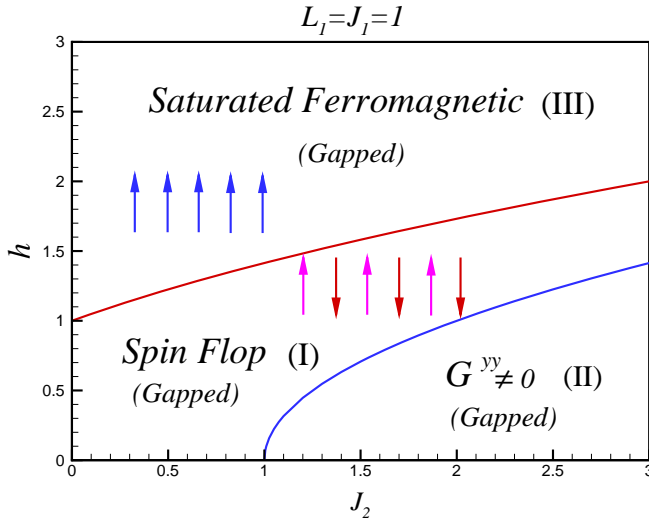


FIG. 1: (Color online) Zero-temperature phase diagram of the extended quantum compass model in the transverse magnetic field for  $L_1 = J_1 = 1$ .

It is useful to recall the zero-temperature phase diagram of the extended compass model in homogenous transverse field, see Fig. (1)<sup>22</sup> (For simplicity we take  $J_1 = L_1 = 1$ ). For  $J_2 < 1$  and small magnetic field  $h < h_0$  (region (I)) the model is in the spin-flop phase (the Néel order along the axis ( $x$ ) which is perpendicular to magnetic field is called spin flop). In this region tuning the magnetic field forces the system to fall into a saturated ferromagnetic (SF) phase above the critical field ( $h_c = h_0$ ). These states exhibit a gap in the excitation spectrum where vanishes at the critical field. In the case of  $J_2 > 1$  there is antiparallel ordering of spin  $y$  component on odd bonds under the lower critical field  $h_{c1} = h_\pi$  (region (II)) and beyond this critical field system goes into a gapped spin-flop phase (region (I)). This spin-flop phase exist for  $h < h_{c2} = h_0$ . Finally, for  $h > h_{c2}$  the ground state is the ferromagnetically polarized state along the magnetic field (region (III)) which exhibits again a gap. These different zero-temperature regions, in particular the quantum phase transitions at  $h_0$  and  $h_\pi$  could be reflected by the magnetocaloric properties at finite temperature<sup>10–13</sup>.

The specific heat of extended quantum compass model in transverse field has been plotted in Figs. (2) and (3) versus temperature ( $T$ ) and magnetic field ( $h$ ) for  $J_2 = 2$

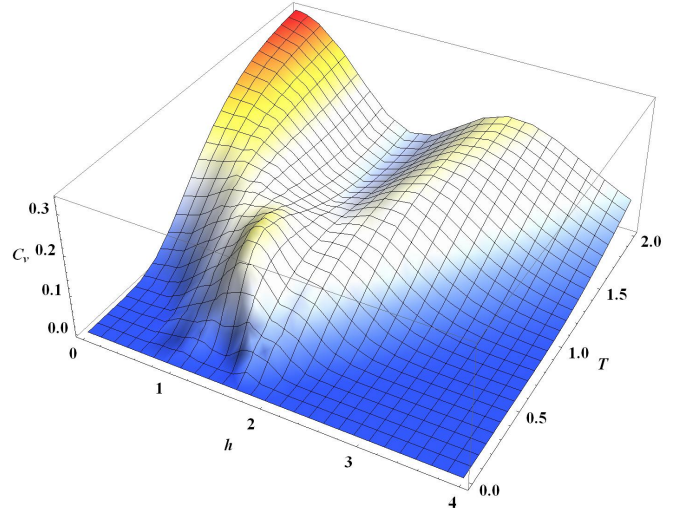


FIG. 2: (Color online) The three-dimensional plot of specific heat of extended quantum compass model in a transverse field versus temperature and magnetic field for  $J_2 = 2$ . For extremely low temperature the maximums of the specific heat happen at  $h_{c1} = 1$  and  $h_{c2} = \sqrt{3}$ .

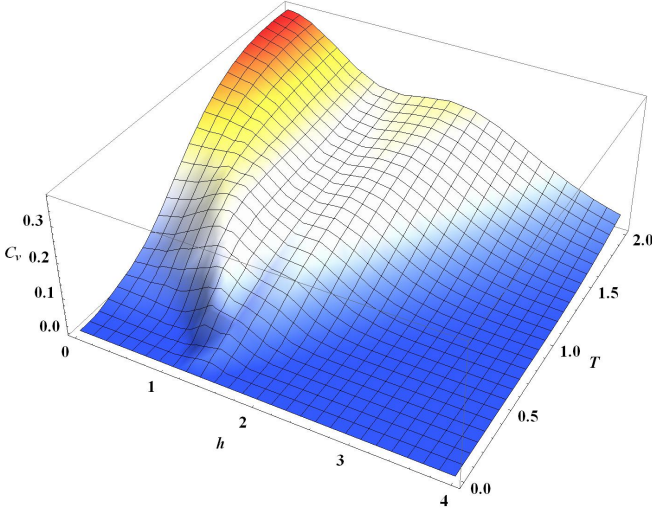


FIG. 3: (Color online) The specific heat of extended quantum compass model in a transverse field versus temperature and magnetic field for  $J_2 = 0.8$ . In this case there is only one maximum at  $h_c = \sqrt{1.8}$  for very low temperature.

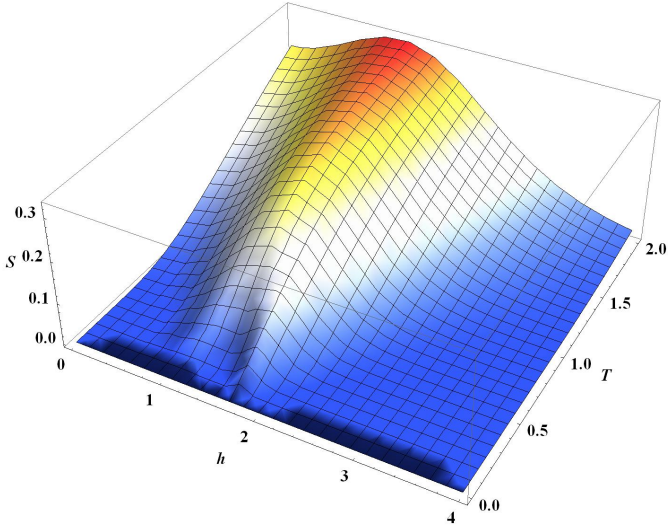


FIG. 4: (Color online) The three-dimensional panorama of entropy of extended quantum compass model in a transverse field versus temperature and magnetic field for  $J_2 = 2$ . The zero-temperature critical fields are signaled by maximum of the entropy at  $h_{c1} = 1$  and  $h_{c2} = \sqrt{3}$  for low temperature.

and  $J_2 = 0.8$  respectively. As it can be seen from Fig. (2), the specific heat reaches its maximums at QCP for extremely low temperatures producing the a small well between two critical fields  $h_{c1} = h_\pi = 1$  and  $h_{c2} = h_0 = \sqrt{3}$ , while there is only one maximum at the critical field  $h_c = h_0 = \sqrt{1.8}$  in Fig. (3).

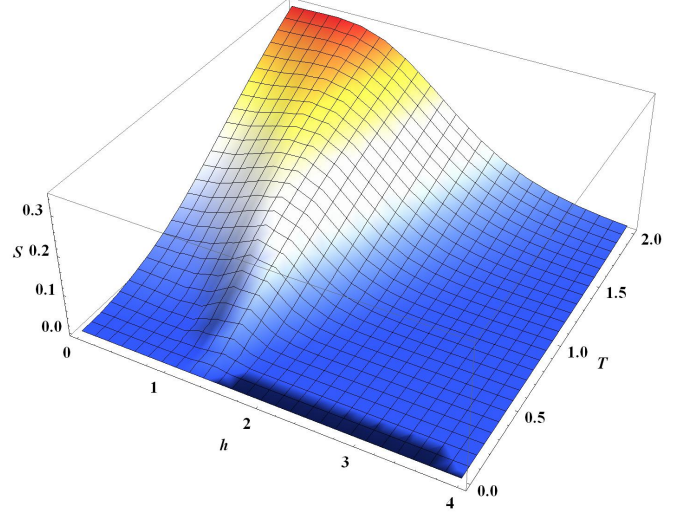


FIG. 5: (Color online) The entropy of extended quantum compass model in a transverse field versus temperature and magnetic field for  $J_2 = 0.8$ . In this case the zero-temperature critical field ( $h_c = \sqrt{1.8}$ ) is specified by maximum of entropy for extremely low temperature.

Figs (4) and (5) show the entropy of the model for  $J_2 = 2$  and  $J_2 = 0.8$ . They manifest that the maximums of the entropy for very low temperature occur at the critical fields just like the specific heat. This accumulation of entropy close QCPs indicates that the system is maximally undecided which ground state to chose. As the temperature is raised, all the characteristic behaviors have been disappeared.

As it was mentioned earlier, a large MCE also characterizes a distinctly different class of materials, where the low temperature properties are governed by pronounced quantum many-body effects. These materials exhibit a field-induced QCPs (a zero-temperature phase transition), and the MCE has been used to study their quantum criticality. The adiabatic demagnetization curves of extended compass model in the transverse field is presented in Figs. (6) and (7) for constant initial value of magnetic field ( $h_i = 3$ ) and several starting temperatures ( $T_i$ ) for  $J_2 = 2$  and  $J_2 = 0.8$ , respectively. The lowest temperatures of an adiabatic process are reached at  $h_1^* < h_{c2} = h_0$  and  $h_2^* > h_{c1} = h_\pi$ . At extremely low temperatures the difference between the demagnetization fields ( $h_1^*, h_2^*$ ) and critical fields ( $h_{c1}, h_{c2}$ ) becomes very small. Clearly, the QCM in transverse field chain cools down to lower temperatures near the second critical field ( $h_0$ ) than the one close to the first critical field ( $h_\pi$ ).

However, the Grüneisen ratio (cooling rate) is noteworthy quantity to specify the second-order transitions since it necessarily diverges near QCPs and the divergent behavior obeys the universal scaling law<sup>26</sup>,

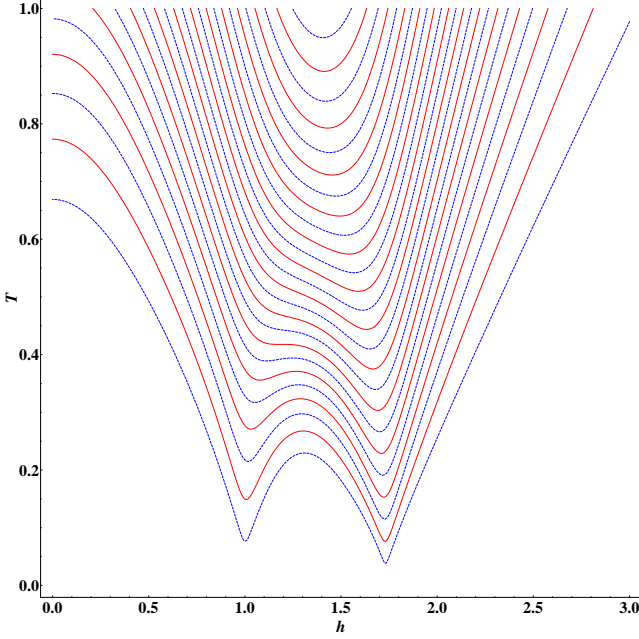


FIG. 6: (Color online) Adiabatic demagnetization curves of the extended quantum compass model in a transverse field for  $J_2 = 2$ . The lowest temperatures occur at zero-temperature critical fields  $h_{c1} = 1$  and  $h_{c2} = \sqrt{3}$ .

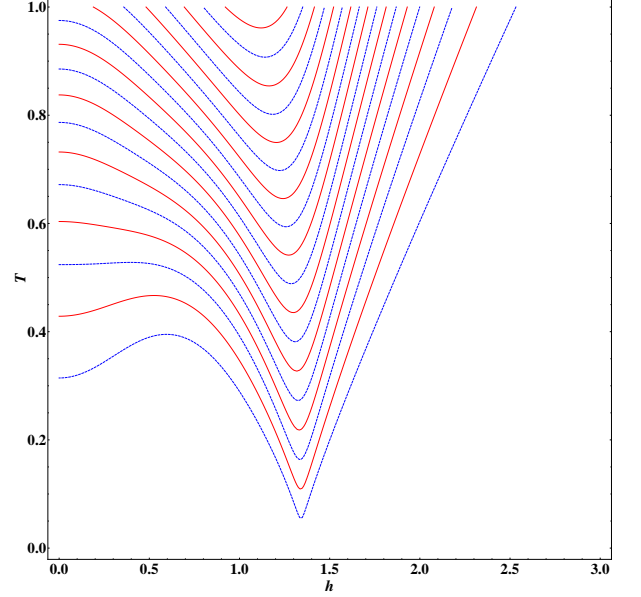


FIG. 7: (Color online) Lines of constant entropy, *i.e.*, adiabatic demagnetization curves of the extended quantum compass model in a transverse field for  $J_2 = 0.8$ . The minimum of isentrop locates at the zero-temperature critical field  $h_c = \sqrt{1.8}$

$$\Gamma_h(T \rightarrow 0, h) = -G_h \frac{1}{h - h_c},$$

where  $G_h$  is a universal amplitude and the value  $G_h = -1$  expected for a  $Z_2$ -symmetry in the one dimension<sup>12</sup>. Moreover, the sign of the Grüneisen ratio changes as entropy accumulates near a quantum critical point<sup>27</sup>. The sign change along with the divergence lead to strong signatures of the Grüneisen parameter near QCPs. The cooling rate of the extended quantum compass model is plotted versus the magnetic field for  $J_2 = 2$  and  $J_2 = 0.9$  in Figs. (8) and (9) respectively. As it can be seen from Fig.(1), for  $J_2 = 2$ , curves show two quantum phase transition at  $h_{c1} = h_\pi = 1$  and  $h_{c2} = h_0 = \sqrt{3}$  and for  $J_2 = 0.9$  show just one quantum phase transition at  $h_c = h_0 = \sqrt{1.9}$ . For low temperature, the quantum phase transition at  $h_{c1} = h_\pi = 1$  and  $h_{c2} = h_0 = \sqrt{3}$  are signaled by sign changes of the cooling rate  $\Gamma_h$  from negative

to positive values upon increasing field, see Fig.(8). However in Fig.(9) the cooling rate  $\Gamma_h$  changes the sign when the magnetic field crosses the QCP ( $h_c = h_0 = \sqrt{1.9}$ ). By increasing the temperature the magnitude of the peaks reduce and all features are washed out which implies that thermal fluctuations are already strong enough to drive the system to the excited state where no quantum phase transition can be seen. In other words, the strong enhancement of the magnetocaloric effect arising from quantum fluctuations near a  $h$ -induced quantum-critical point can be used for finding an efficient and flexible high performance magnetic cooling over an extended temperature range.



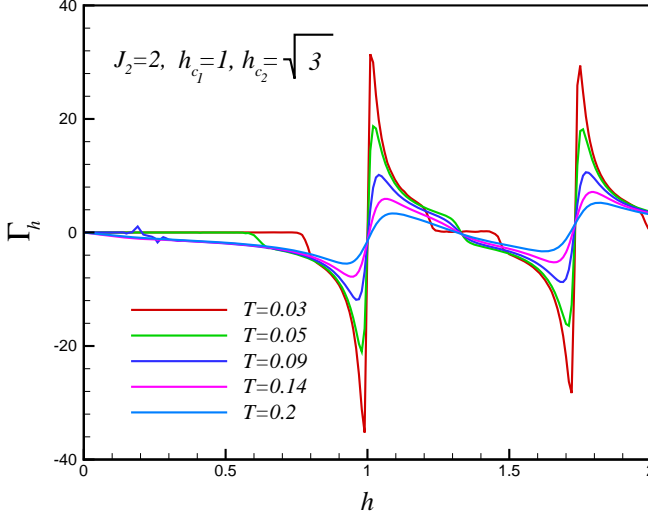


FIG. 8: (Color online) Magnetic cooling rate ( $\Gamma_h$ ) versus magnetic field for different values of temperature for  $J_2 = 2$ .

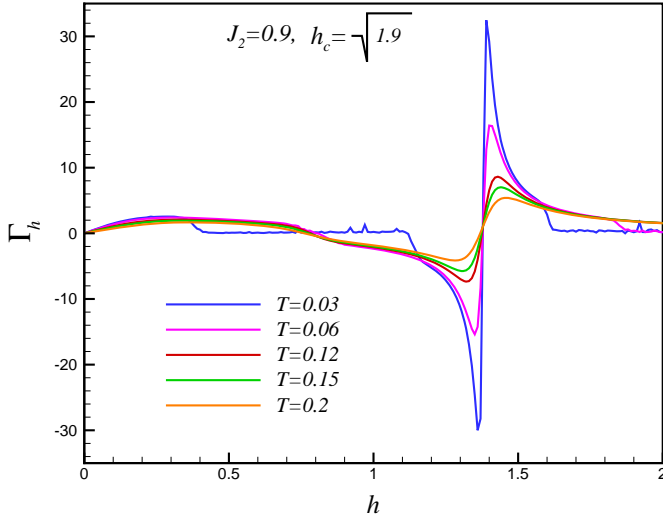


FIG. 9: (Color online) The variations of cooling rate ( $\Gamma_h$ ) with magnetic field for different values of temperature for  $J_2 = 0.9$ .

#### IV. EXTENDED QUANTUM COMPASS MODEL ( $h_1 = h_2 = 0$ )

The complete phase diagram of the extended compass model has been reported in Refs. [21] and [28]. They have shown that this model is always gapful except at the critical line. The multicritical point located on the intersection of the first-order ( $J_1/L_1 = 0$ ) and second order transition ( $J_2/L_1 = 1$ ) lines (For simplicity we take  $L_1 = 1$ ).

The specific heat of extended quantum compass model versus temperature ( $T$ ) and the parameter deriving the

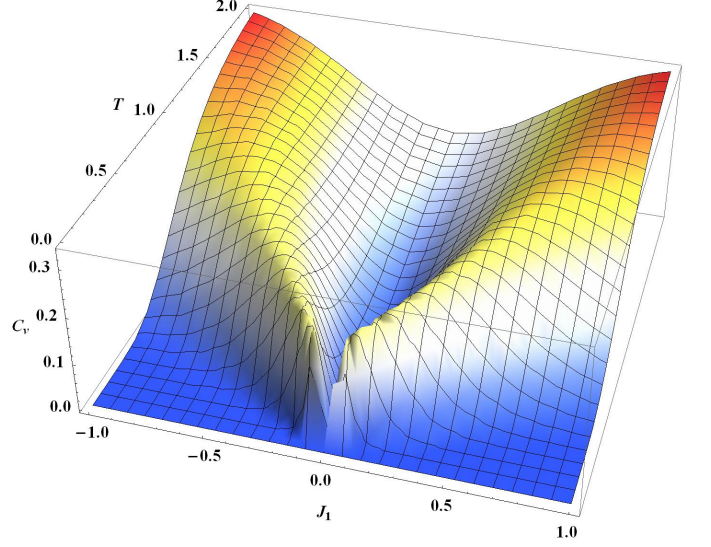


FIG. 10: (Color online) The three-dimensional plot of specific heat of extended quantum compass model versus temperature and the parameter which derives the first-order transition ( $J_1$ ) for  $J_2 = 2$ .

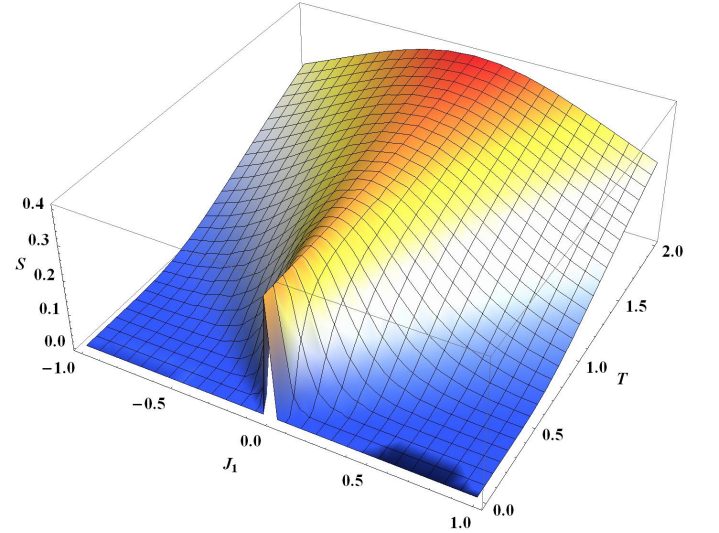


FIG. 11: (Color online) The three-dimensional panorama of entropy of extended quantum compass model versus temperature and  $J_1$  for  $J_2 = 2$ .

first-order transition ( $J_1$ ) is plotted in Fig. (10). As it is clear, the minimum of the specific heat occurs on the first order transition line ( $J_1 = 0$ ) for any arbitrary temperature. Fig. (11) shows the three-dimensional panorama of the entropy versus  $T$  and  $J_1$  which manifests that the maximum of the entropy lies on the first order transition

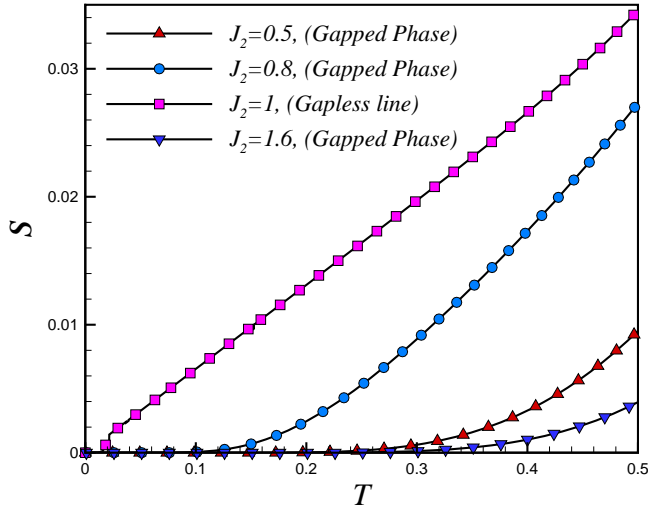


FIG. 12: (Color online) Entropy of the extended quantum compass model versus  $T$  for  $J_2 = 0.5$ ,  $J_2 = 0.8$ ,  $J_2 = 1$  and  $J_2 = 1.6$ . Entropy on the gapless line ( $J_2 = 1$ ) shows the linear behavior.

line ( $J_1 = 0$ ). It is worthy to mention that the system is gapful on this line where the degenerate ground-state separates from the excited state. So, the prominent characteristic of the specific heat and entropy on the first-order transition line inherited from the existence of a gap.

However, the maximum entropy and specific heat falls out from the second order transition line ( $J_2 = 1$ ) for extremely low temperatures. On this line the system is gapless and entropy is linear in  $T$  ( $S \propto T$ ) for low temperatures while in the gapped cases ( $J_2 \neq 1$ ) we expect activated behavior<sup>16</sup>

$$S \propto \exp(-\Delta/T)$$

where  $\Delta$  is gap in the excitation spectrum. The low temperature behavior of the entropy is plotted in Fig. (12) which verifies the linear and exponential behaviors of the entropy on the transition line and gapped phases. The asymptotic behavior is  $S \rightarrow 0$  for  $T \rightarrow 0$  in all cases. The cooling rate is plotted versus  $J_1$  and  $J_2$  in Figs. (13) and (14), respectively.

The cooling rate dependence on  $J_1$  is plotted in Fig. (13) for different values of temperature. It is shown that the first-order transitions are signaled by very sharp and pronounced positive and negative peaks at the transition point ( $J_1 = 0$ ). Further the only difference between the curves, which correspond to different temperatures, is difference in the strength of the peaks. Fig. (14) shows the variations of cooling rate with  $J_2$ . The QCP pinpointed by sign changes of the cooling rate  $\Gamma_{J_2}$  from negative to positive values upon increasing  $J_2$ . The magnitude of the peaks grows rapidly with decreasing the temperature.

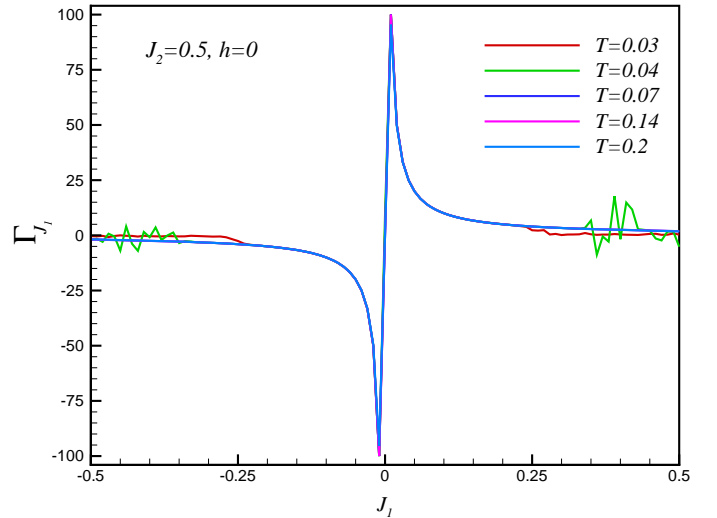


FIG. 13: (Color online) Cooling rate ( $\Gamma_{J_1}$ ) versus  $J_1$  for different values of temperature,  $J_2 = 2$ .

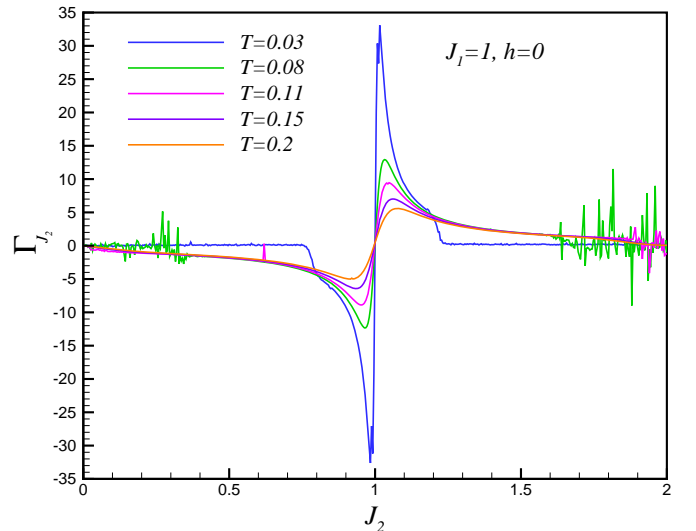


FIG. 14: (Color online) The variations of cooling rate ( $\Gamma_{J_2}$ ) with the parameter that derives the second-order transition ( $J_2$ ) for different values of temperature,  $J_1 = 1$ .

## V. SUMMARY AND CONCLUSIONS

In this paper we have studied the thermodynamic properties of the one dimensional extended quantum compass model in peresence/absent of transverse field. We have presented the specific heat, entropy, adiabatic demagnetization curves and Grüneisen parameter, which is proportional to the magnetocaloric effect, as a function of the external magnetic field on the thermodynamic limit and at finite temperatures. We have used the exact result for the entropy to illustrate that field-

induced quantum phase transitions give rise to maxima of the low-temperature entropy, or equivalently minima of the isentropes. This leads to cooling during adiabatic (de)magnetization processes where the lowest temperature is reached close to the quantum phase transition. As a consequence, we found a large positive (negative) values of the normalized cooling rate for magnetic fields slightly above (below) the critical fields. The general features of the entropy should not depend on the specific choice of the magnetic field  $h$  as control parameter and

indeed similar behavior is found as a function of the exchange couplings. The low-temperature asymptotics of the entropy  $S$  is exponentially activated in the gapped phases and is linear in  $T$  on the second order transition line.

## References

- 
- \* jafari@iasbs.ac.ir, jafari@nss.co.ir
- <sup>1</sup> E. Warburg, Ann. Phys. Chem. **13**, 141 (1881).
  - <sup>2</sup> K. A. Gschneider, Jr., V. K. Pecharsky, and A. O. Tsokol, Rep. Prog. Phys. **68**, 1479 (2005).
  - <sup>3</sup> A. M. Tishin and Y. I. Spichkin, *The Magnetocaloric Effect and its Applications*, (Institute of Physics Publishing, Bristol, 2003).
  - <sup>4</sup> D. P. MacDougall, W. F. Giauque, Phys. Rev. **43** 768 (1933).
  - <sup>5</sup> A. S. Oja and O. V. Lounasmaa, Rev. Mod. Phys. **69**, 1 (1997).
  - <sup>6</sup> P. Strehlow, H. Nuzha, and E. Bork, J. Low Temp. Phys. **147**, 81 (2007).
  - <sup>7</sup> J. C. Bonner and J. F. Nagle, Phys. Rev. A **5**, **2293** (1972).
  - <sup>8</sup> L. Zhu, M. Garst, A. Rosch, Q. Si, Phys. Rev. Lett. **91**, 066404 (2003).
  - <sup>9</sup> M. Garst, A. Rosch, Phys. Rev. B. **72**, 205129 (2005).
  - <sup>10</sup> A. Honecker, S. Wessel, Condensed Matter Physics. **12**, 399 (2009).
  - <sup>11</sup> M. E. Zhitomirsky, H. Tsunetsugu, Phys. Rev. B. **70** 100403 (2004).
  - <sup>12</sup> M. E. Zhitomirsky and A. Honecker, J. Stat. Mech.: Theor. Exp. P07012 (2004).
  - <sup>13</sup> A. Honecker, S. Wessel, Physica B. **378**, 1098 (2006).
  - <sup>14</sup> B. Schmidt, P. Thalmeier, N. Shannon, Phys. Rev. B. **76** 125113 (2007).
  - <sup>15</sup> M. S. S. Pereira, F. A. B. F. de Moura, M. L, Phys. Rev. B. **79** 054427 (2009).
  - <sup>16</sup> C. Trippé, A. Honecker, A. Klümper, V. Ohanyan, Phys. Rev. B **81**, 054402 (2010).
  - <sup>17</sup> K. I. Kugel and D. I. Khomskii, Sov. Phys. JETP **37**, 725 (1973).
  - <sup>18</sup> G. Jackeli and G. Khaliullin, Phys. Rev. Lett. **102**, 017205 (2009).
  - <sup>19</sup> W. Brzezicki, J. Dziarmaga, and A. M. Oleś, Phys. Rev. B **75**, 134415 (2007).
  - <sup>20</sup> W. Brzezicki, J. Dziarmaga, and A. M. Oleś, Acta Phys. Pol. A **115**, 162 (2009).
  - <sup>21</sup> Erik Eriksson and Henrik Johannesson, Phys. Rev. B **79**, 224424 (2009).
  - <sup>22</sup> R. Jafari, e-print arXiv:1101.3673v1.
  - <sup>23</sup> E. Lieb, T. Schultz, and D. Mattis, Ann. Phys. (N.Y.) **16**, 407 (1961); E. Barouch and B. M. McCoy, Phys. Rev. A **3**, 786 (1971); J. B. Kogut, Rev. Mod. Phys. **51**, 659 (1979); J. E. Bunder and R. H. McKenzie, Phys. Rev. B **60**, 344 (1999).
  - <sup>24</sup> J. H. H. Perk, H. W. Capel and M. J. Zuilhof, Physica **81A** 319 (1975).
  - <sup>25</sup> K. Sengupta, D. Sen, and S. Mondal, Phys. Rev. Lett. **100**, 077204 (2008); S. Mondal, D. Sen, and K. Sengupta, Phys. Rev. B **78**, 045101 (2008).
  - <sup>26</sup> R. Kuchler, N. Oeschler, P. Gegenwart, T. Cichorek, K. Neumaier, O. Tegus, C. Geibel, J. A. Mydosh, F. Steglich, L. Zhu, and Q. Si, Phys. Rev. Lett. **91**, 066405 (2003).
  - <sup>27</sup> J. Sznajd, Phys. Rev. B **78**, 214411 (2008).
  - <sup>28</sup> S. MahdaviFar, Eur. Phys. J. B **77**, 77-82 (2010).